Proceeding of the IEEE
International Conference on Robotics and Biomimetics
Dali, China, December 2019

BioTetra: A Bioinspired Multi-Rotor Aerial Vehicle*

Binbin Li and Duo Wang.
School of Electrical Engineering
Southwest Jiaotong University
Chengdu, Sichuan Province, China
{*bk20123885, yj2019200454*}*@my.swjtu.edu.cn*

Lei Ma*
School of Electrical Engineering
Southwest Jiaotong University
Chengdu, Sichuan Province, China
malei@swjtu.edu.cn

***Abstract*— Applications of multi-rotor aerial robots are progressively expanding into various industries. However, due to its actuators configuration, standard multi-rotor vehicles flexibility is greatly limited. In this manuscripts, we proposed a bioinspired multi-rotor aerial vehicle, called BioTetra, a class of aircraft capable of vector-flying and omnidirectional movement. The BioTetra vehicle, which finds inspiration in the configuration layout of the organic molecules(CH_4), exploits its stability of the regular tetrahedral structure. The new abilities of the BioTetra vehicle not only improve flight efficiency, but also expand the reachable set. First, the mechanical design with regular tetrahedron configuration layout is introduced. Then, a quaternion-based attitude controller is designed to track a full pose trajectory in space. The virtual simulation of the aerial vehicle verifies the feasibility of the new structure and the effectiveness of the control strategy.**

***Index Terms*— Aerial vehicle, omni-directional movement, vector-flying, over-actuated system.**

I. Introduction

The emergence of aerial robots, popularly known as multi-rotor vehicles, provides major opportunities for applications in various industries, such as as agriculture, searching and rescuing missions, mapping, navigation, war spying and in production and manufacturing system(e.g.,[1]-[4]). Although the uses of aerial robots are increasing, maneuvering flight, constrained actuators configuration still remains a challenge.

In order to improve the performance of standard multi-rotor vehicles, all propellers disks are generally aligned in a single plane. The advantage of this structural configuration is that the structural design is simplified, but the translational and rotational dynamics are coupled to each other. Therefore, these standard multi-rotor vehicles are under-actuated systems, that is, unable to independently control their position and attitude. The inability of standard multi-rotor vehicles to independently control their moment and thrust limits their reachable set. So, standard multi-rotor vehicles can only track a 4-D (altitude, roll, pitch and yaw) trajectory in three dimensions space.

* This work is supported by the National Natural Science Foundation of China under Grant U1730105.

* Lei Ma is the corresponding author(e-mail: malei@swjtu.edu.cn).

To increase performance criteria such as robustness, mobility or reachable set, various new ideas have been applied to the design of novel aerial robots. One traditional improvement is to change the mounting position or direction of the actuator(e.g., [5]-[10]). For instance, omni-directional aerial vehicle have been developed with optimized distributed rotors to maximizes the vehicles agility in any direction [5]. In [6], a fully-actuated flying platform with the ability of omni-directional movement is also proposed, it can assume arbitrary motion in SE(3) or generate arbitrary control wrench in SE(3). In [8] and [9], multi-rotor aerial robots with tilting propellers are analyzed. By applying tilt angles to change the thrust direction with respect to the body frame, these aerial vehicle can only improve the performance of the aircraft in some way, such as mobility or omni-directionality.

Fig. 1. Photograph of the BioTetra vehicle: four 2-DOF tilting module embedded at four vertices of a regular tetrahedron.

Another popular improvement is to look for design inspiration from the biosphere(e.g., [11]-[13]). In [11], a dual-rotor-embedded multilink robot with the ability of multi-degree-of-freedom aerial transformation is introduced. The novel aerial vehicle looks like a dragon, it can control the full pose in three-dimensional space regarding the center of gravity. In [12], an origami structure inspired by insect wings used as an element of a quadrotor frame that can avoid permanent damage. In [13], a class of micro air vehicle with the capability of forceful tugging up to 40 times their mass

978-1-7281-6321-5/19//$31.00 ©2019 IEEE

while adhering to a surface. This class of aerial vehicle is inspired by the prey transportation strategy of wasps that can rapidly traverse cluttered three-dimensional terrain and exert forces that affect human-scale environments.

In this paper, we introduce a novel multi-rotor aerial vehicle capable of vector-flying and omni-directional movement(see Fig.1). The translational dynamics of the aerial vehicle is decoupled from the rotational dynamics. So, the vehicle can track a 6-D trajectory in space. The design idea of the aerial vehicle is inspired by the molecular structure(CH_4), exploits its stability of the regular tetrahedral structure. The advantage of this configuration structural is that the aerial vehicle is extremely stable in any attitude. At the same time, when any actuator fails, the aerial vehicle can quickly return to a stable state.

The rest of this paper is organized as follows: the approach overview, 2-DOF tilting modules configuration and flight modes analysis are introduced in Section II. Section III presents the dynamics model of the proposed aerial vehicle based on quaternion. Section IV represents the control strategy to track arbitrary position and attitude. The simulation results are shown in Section V.

II. Approach Overview

In nature, many organic molecules have a regular tetrahedral structure which is the strongest and most stable molecular structure. In the methane molecule CH_4(Fig.2a), for instance, the carbon atom is located at the center of a tetrahedron with the four hydrogen atoms located at the four apexes of the tetrahedron. Thus, any three hydrogen atoms are not collinear and can form a plane. According to the stability principle of the tilting tri-rotor aircraft, three non-collinear rotors and one tail rudder can achieve attitude stabilization control[14].

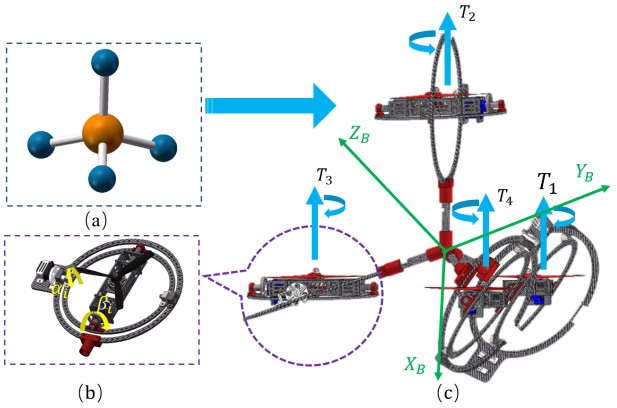

Fig. 2. Concept of the aerial robot: (a) the tetrahedral carbon's configuration;(b) 2-DOF tilting module; (c) BioTetra vehicle.

According to the above analysis, if an aerial vehicle with a regular tetrahedral configuration layout and can provide vector thrust (controllable both magnitude and direction) at each vertex, the vehicle can be equivalent to four tilting tri-rotors aircraft. The benefit of such configuration is that when any one vertex fails, the forces of the remaining three vertices can be redistributed, avoiding the risk of crash. Inspired by this, we designed a 2-DOF tilting rotor module that can independently control the magnitude and direction of the force(see Fig.2b). Finally, the aircraft is designed as shown in Fig.2c, four 2-DOF tilting rotor modules are mounted at the vertexes of a regular tetrahedron, respectively. Then, let $\boldsymbol{p}_i$ be the origin of the propeller frames $\mathcal{F}_{Pi}$, it follows from Fig. 2 that the position matrix $\boldsymbol{P}$ is given by

$$\boldsymbol{P} = l \begin{bmatrix} \frac{\sqrt{6}}{3} & 0 & \frac{-\sqrt{6}}{3} & 0 \\ 0 & \frac{\sqrt{6}}{3} & 0 & \frac{-\sqrt{6}}{3} \\ \frac{-\sqrt{3}}{3} & \frac{\sqrt{3}}{3} & \frac{-\sqrt{3}}{3} & \frac{\sqrt{3}}{3} \end{bmatrix} \tag{1}$$

where $\boldsymbol{P} = [\boldsymbol{p}_1, \boldsymbol{p}_2, \boldsymbol{p}_3, \boldsymbol{p}_4]$, l is the distance between the vehicle's center of mass and the center of tilting module.

Let $\boldsymbol{O} = [\boldsymbol{o_1}, \boldsymbol{o_2}, \boldsymbol{o_3}, \boldsymbol{o_4}]$ denote the orientation matrix that describes the thrust direction with respect to the body frame. It can be written as

$$\boldsymbol{O} = \begin{bmatrix} s(\beta_1+\gamma)c(\alpha_1) & s(\alpha_2) & -s(\beta_3+\gamma)c(\alpha_3) & -s(\alpha_4) \\ -s(\alpha_1) & c(\alpha_2)s(\beta_2-\gamma) & s(\alpha_3) & -s(\beta_4-\gamma)c(\alpha_4) \\ c(\beta_1+\gamma)c(\alpha_1) & c(\alpha_2)c(\beta_2-\gamma) & c(\beta_3+\gamma)c(\alpha_3) & c(\beta_4-\gamma)c(\alpha_4) \end{bmatrix} \tag{2}$$

with γ is the angle between body Y-axis and the i-th arms, and $\cos(\gamma) = \frac{\sqrt{6}}{3}, \sin(\gamma) = \frac{\sqrt{3}}{3}$.

The principle of the 2-DOF tilting rotor module is shown in Fig.3. Two servo motors control the thrust to rotate about the X_{Pi}-axis(α_i) and the Y_{Pi}-axis(β_i), respectively. The thrust f_i(unit:N) and torque τ_i(unit:$N \cdot m$) generated by the rotor can be written as

$$f_i = k_1 {\varpi_i}^2 \tag{3}$$

$$\tau_i = c_2 f_i = k_1 k_2 {\varpi_i}^2 \tag{4}$$

where k_1, k_2 are constants that can be determined by experiments. ϖ_i represents the angular velocity of the $i-th$ rotor

The BioTetra vehicle consists of four 2-DOF tilting rotor modules, the thrust $\boldsymbol{f}$ and torque $\boldsymbol{\tau}$ acting on the aircraft can be written as

$$\boldsymbol{f} = \sum_{i=1}^{4} f_i \boldsymbol{o_i}, \tag{5}$$

$$\boldsymbol{\tau} = \sum_{i=1}^{4} f_i (\boldsymbol{p}_i \times \boldsymbol{o_i}) + \tau_i \boldsymbol{o_i} \tag{6}$$

where $\boldsymbol{o_i}$ is the propeller disk normal. It should be noted that the influence of air resistance on the aircraft is neglected. The first term in Eq.6 denotes the moment by reason of the off-center mounting of the propellers, while the second term denotes the reaction moment generated by the aerodynamic drag of the propeller. Since the latter term is typically an order of magnitude smaller, this term will be omitted in the rest of analysis. The summation of force and torque acting on the aerial vehicle can then be expressed as

$$\begin{bmatrix} \boldsymbol{f} \\ \boldsymbol{\tau} \end{bmatrix} = \begin{bmatrix} \boldsymbol{O} \\ \boldsymbol{P} \times \boldsymbol{O} \end{bmatrix} \boldsymbol{f}_r \tag{7}$$

where $\boldsymbol{f}_r = [f_1, f_2, f_3, f_4]$.

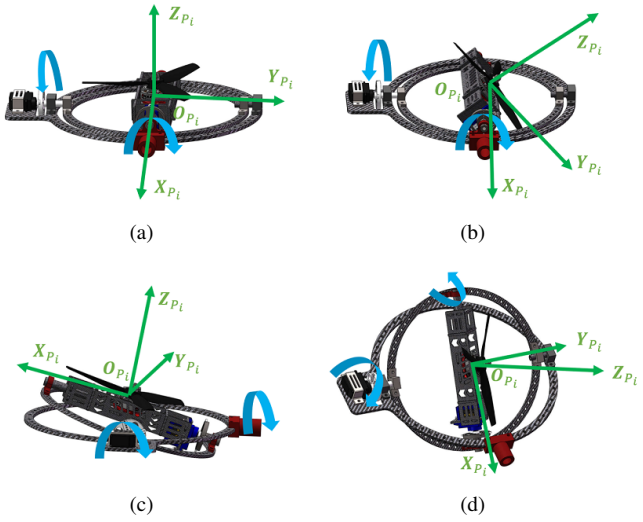

Fig. 3. ith 2-DOF tilting module visualizing the body frame $\mathcal{F}_{P_i}$. (a),$\alpha_i = 0°$, $\beta_i = 0°$. (b),$\alpha_i = 30°$, $\beta_i = 0°$. (c),$\alpha_i = 0°$, $\beta_i = 10°$. (d),$\alpha_i = 10°$, $\beta_i = 10°$.

It is proven that the moment of inertia merely reduces to a multiple of the unit tensor for solids that have at least two n-fold rotational axes ($n \geq 3$)[15]. Assuming that the moment of inertia is mainly determined by the rotor positions and that the 2-DOF tilting modules can be approximated by point masses. These point masses are the vertices of regular tetrahedron solids. Consequently, the set of rotor positions satisfy the above criterion. Thus, the moment of inertia is rotationally invariant. The inertia tensor described in frame $\mathcal{F}_H$ can be expressed as J.

III. Dynamics

In this section, according to Newton-Eulerian's law, the dynamic model of the BioTetra vehicle is established with the angular velocities of the rotor and the angle of the servo motors as inputs. Due to the spatial three-dimensional structure of the aerial robot and the tight layout of the tilting rotor module, complex aerodynamic effects (such as mutual interference between the rotors and rotation of the servo motor in the tilting rotor module) will have a significant impact on the dynamics of the aircraft. Therefore, modeling the over-actuated aerial vehicle is a very challenging task.

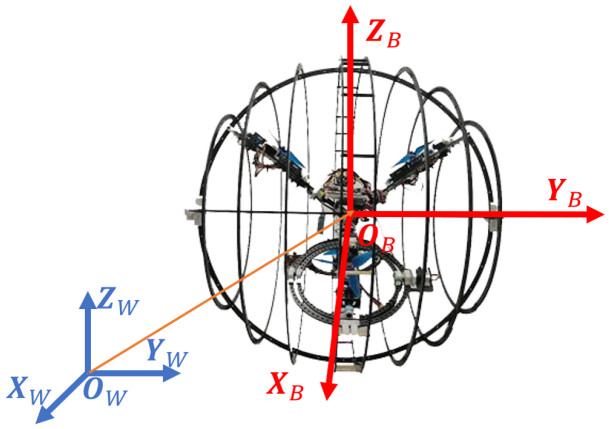

Fig. 4. Illustration of the proposed BioTetra vehicle design with its body-fixed coordinate frame $\mathcal{F}_B$. The overall center of mass is assumed to be in the body-fixed coordinate frame center. The vehicle is actuated by four propellers.

In Fig.4, $\boldsymbol{O}_B$ is the center of gravity of the BioTetra vehicle. Let $\mathcal{F}_W : \{\boldsymbol{O}_W; \boldsymbol{X}_W, \boldsymbol{Y}_W, \boldsymbol{Z}_W\}$ denote the right handed inertial world frame, $\mathcal{F}_B : \{\boldsymbol{O}_B; \boldsymbol{X}_B, \boldsymbol{Y}_B, \boldsymbol{Z}_B\}$ denote the right handed body frame to the BioTetra vehicle, $\mathcal{F}_{P_i} : \{\boldsymbol{O}_{P_i}; \boldsymbol{X}_{P_i}, \boldsymbol{Y}_{P_i}, \boldsymbol{Z}_{P_i}\}$, $i = 1, ..., 4$, denote the frame associated to the ith 2-DOF tilting module.

The orientation of the frame $\mathcal{F}_B$ with respect to the world inertial frame $\mathcal{F}_W$ is defined as ${}^W\mathrm{R}_B \in \mathbf{SO}(3)$, and ${}^B\mathrm{R}_{P_i}$ is the orientation of the ith propeller with respect to the body-fixed frame. Let $\alpha_i \in \mathbb{R}$ denote the propeller tilting angle about axis $\boldsymbol{X}_{P_i}$, and $\beta_i \in \mathbb{R}$ the propeller tilting angle about axis $\boldsymbol{Y}_{P_i}$.

Let the generalized coordinates of the BioTetra vehicle be expressed by

$$\boldsymbol{\chi} = (x, y, z, \psi, \theta, \phi) \tag{8}$$

where $\xi = (x, y, z)^T$ denotes the position vector of the center of mass of the aerial vehicle to the inertial frame $\mathcal{F}_W$. The orientation vector of the aerial vehicle with respect to the inertial world frame is expressed by $\eta = (\psi, \theta, \phi)$, where ψ is yaw angle around the axis $\boldsymbol{Z}_W$, θ is pitch angle around $\boldsymbol{Y}_W$ and ϕ is roll angle around $\boldsymbol{X}_W$.

Similarly, let ${}^B\mathrm{O}_{Pi}$ be the orientation vector. The rotation from frame $\mathcal{F}_{Pi}$ to $\mathcal{F}_B$ can be expressed as

$${}^B\mathrm{O}_{Pi} = \mathrm{R}_{Z_B}^{-1}((i-1)\frac{\pi}{2})\mathrm{R}_{Y_B}^{-1}(\beta_i + (-1)^{i-1}\gamma)\mathrm{R}_{X_B}^{-1}(\alpha_i) \tag{9}$$

Since the direction of the thrust with respect to the frame $\mathcal{F}_{Pi}$ is fixed , it can be expressed as ${}^{Pi}\mathrm{O}_{Pi} = [0 \quad 0 \quad 1]^T$. Define the initial state as shown in Fig. 4.

The relationship between the derivative of the quaternion and the vehicle's angular velocity is expressed as

$$\dot{\mathbf{q}} = \frac{1}{2}\mathbf{q} \otimes \begin{bmatrix} 0 \\ {}^{b}\boldsymbol{\omega} \end{bmatrix} = \begin{bmatrix} -\frac{1}{2}\mathbf{q}_{1:3}^{T} \cdot {}^{b}\boldsymbol{\omega} \\ \frac{1}{2}(q_0\mathbf{I}_3 + [\mathbf{q}_{1:3}]_{\times}) \cdot {}^{b}\boldsymbol{\omega} \end{bmatrix} \tag{10}$$

where ${}^{b}\boldsymbol{\omega}$ denotes the robot's body rates, and $[\mathbf{q}_{1:3}]_{\times}$ denotes the skew-matrix of $\mathbf{q}_{1:3}$

$$[\mathbf{q}_{1:3}]_{\times} = \begin{bmatrix} 0 & -q_3 & q_2 \\ q_3 & 0 & -q_1 \\ -q_2 & q_1 & 0 \end{bmatrix} \tag{11}$$

Dynamics of the vehicle are then described by Newton-Euler equations:

$$m\ddot{\boldsymbol{p}} = m \begin{bmatrix} 0 \\ 0 \\ -g \end{bmatrix} + \mathrm{R}(q_b^e){}^{b}\boldsymbol{f} \tag{12}$$

$$\boldsymbol{\tau}_b = \boldsymbol{J}\dot{\boldsymbol{\omega}} + \boldsymbol{\omega} \times \boldsymbol{J}\boldsymbol{\omega} \tag{13}$$

where m is the total mass of the aerial vehicle and g is the scalar gravitational acceleration. $\mathbf{q}_{pi}^{e}$ denotes the rotation quaternion that maps a vector from the ith 2-DoF tilting module frame $\mathcal{F}_{P_i}$ to the inertial frame $\mathcal{F}_W$.

IV. Control Design

To achieve full pose trajectory tracking, unit quaternion is used to define the angular pose of the aerial vehicle.

The quaternion is expressed as $\boldsymbol{q} = (q_0, \boldsymbol{\eta}) \in \mathbb{R}^4$, where $q_0 \in \mathbb{R}$ represents the scalar part, $\boldsymbol{\eta} = [q_1, q_2, q_3]^T$ represents the vector part. And with

$$\boldsymbol{q} = q_0 + q_1\boldsymbol{i} + q_2\boldsymbol{j} + q_3\boldsymbol{k} \tag{14}$$

with $q_0^2 + q_1^2 + q_2^2 + q_3^2 = 1$, $\boldsymbol{i}, \boldsymbol{j}, \boldsymbol{k}$ denote the unit vector, respectively. The rotational matrix $\mathbf{R} = [R_{ij}]$ is used to describe the vehicle coordinate $\mathcal{F}_B$ with respect to the world coordinate $\mathcal{F}_W$, the corresponding quaternion is

$$\begin{cases} q_0 = \frac{1}{2}\sqrt{1 + R_{11} + R_{22} + R_{33}} \\ q_1 = \frac{R_{32} - R_{23}}{4q_0} \\ q_2 = \frac{R_{13} - R_{31}}{4q_0} \\ q_3 = \frac{R_{21} - R_{12}}{4q_0} \end{cases} \tag{15}$$

The thrust of the i-th propeller may be decomposed into three contributions, it can be written as:

$$\begin{cases} P_i^a = f_i c_{\alpha i} s_{\beta i} \\ P_i^b = f_i s_{\alpha i} \\ P_i^c = f_i c_{\alpha i} c_{\beta i} \end{cases} \tag{16}$$

where, $\alpha_i = \arcsin(P_i^a, f_i)$, $\beta_i = \arctan 2(P_i^a, P_i^c)$. Then, the input vector $\boldsymbol{u}$ is given by

$$\boldsymbol{u} = [P_1^a, P_1^b, P_1^c, P_2^a, P_2^b, P_2^c, P_3^a, P_3^b, P_3^c, P_4^a, P_4^b, P_4^c]^{\mathrm{T}} \tag{17}$$

The Eq.7 can be written as following formula:

$$\begin{bmatrix} \boldsymbol{f} \\ \boldsymbol{\tau} \end{bmatrix} = \mathbf{A}(\boldsymbol{\alpha}, \boldsymbol{\beta}) \cdot \boldsymbol{u} \tag{18}$$

where $\mathbf{A}(\boldsymbol{\alpha}, \boldsymbol{\beta}) = [\mathbf{B}_f, \mathbf{B}_m]^T \in \mathbb{R}^{6\times 12}$ is the matrix that maps the actuators to force and torque, the rows represents the degree of freedom, while the column represents the aerial vehicle actuator units. Rank of the matrix $\mathbf{A}(\boldsymbol{\alpha}, \boldsymbol{\beta})$ determines the controllability of the aerial vehicle, which is an import fact for the motion planning and control design. The matrix $\mathbf{B}_f$ and $\mathbf{B}_m$ is given by:

$$\mathbf{B}_f = \begin{bmatrix} -1 & 0 & 0 & 0 & -1 & 0 \\ 0 & -1 & 0 & -1 & 0 & 0 \\ 1 & 0 & 0 & -1 & 0 & 0 \\ -1 & 0 & 0 & 0 & 1 & 0 \\ 0 & 1 & 0 & -1 & 0 & 0 \\ 1 & 0 & 0 & -1 & 0 & 0 \end{bmatrix} \boldsymbol{u} \tag{19}$$

$$\mathbf{B}_m = l \begin{bmatrix} 0 & -k_2 & 0 & k_2 & 0 & -1 \\ k_2 & 0 & -1 & 0 & -k_2 & 0 \\ 0 & -1 & 0 & 0 & k_2 & 0 \\ 0 & k_2 & 0 & -k_2 & 0 & 1 \\ k_2 & 0 & 1 & 0 & k_2 & 0 \\ 0 & -1 & 0 & 0 & 1 & 0 \end{bmatrix} \boldsymbol{u} \tag{20}$$

Then, the dynamic model can be rewritten as

$$\begin{cases} m\ddot{\mathbf{p}} = \mathbf{R}\mathbf{B}_f\boldsymbol{u} + m\mathbf{g} \\ \mathbf{J}\dot{\omega} = \mathbf{B_m}\boldsymbol{u} - \boldsymbol{\omega} \times \boldsymbol{J}\boldsymbol{\omega} \end{cases} \tag{21}$$

Then we define the matrix $\mathbf{M}, \mathbf{Q}$ and vector $\boldsymbol{h}$ as

$$\mathbf{M} = \begin{bmatrix} m\mathbf{I}_3 & \mathbf{0}_3 \\ \mathbf{0}_3 & \mathbf{J} \end{bmatrix}, \mathbf{Q} = \begin{bmatrix} \mathbf{R}\mathbf{B}_f \\ \mathbf{B}_m \end{bmatrix}, \boldsymbol{h} = \begin{bmatrix} m\mathbf{g} \\ -\boldsymbol{\omega} \times \boldsymbol{J}\boldsymbol{\omega} \end{bmatrix} \tag{22}$$

where $\mathbf{0_3}$ is a 3×3 null matrix. Then, the translational dynamics model can be written as

$$\mathbf{M} \begin{bmatrix} \ddot{\boldsymbol{p}} \\ \dot{\boldsymbol{\omega}} \end{bmatrix} = \mathbf{Q}\boldsymbol{u} + \boldsymbol{h} \tag{23}$$

Let define $\boldsymbol{y}_p, \boldsymbol{y}_\omega$ as the new control input, the control law is designed as

$$\boldsymbol{u} = \mathbf{Q}^{\dagger} \left(\mathbf{M} \begin{bmatrix} \mathbf{y}_p \\ \mathbf{y}_\omega \end{bmatrix} - \boldsymbol{h} \right) \tag{24}$$

with

$$\begin{bmatrix} \ddot{\boldsymbol{p}} \\ \dot{\boldsymbol{\omega}} \end{bmatrix} = \begin{bmatrix} \boldsymbol{y}_p \\ \boldsymbol{y}_\omega \end{bmatrix} \tag{25}$$

where $\mathbf{Q}^{\dagger}$ is the pseudo-inverse matrix of matrix $\mathbf{Q}$.

Let $\{\boldsymbol{p}_d, \dot{\boldsymbol{p}}_d, \ddot{\boldsymbol{p}}_d\}$ denote the desired position, and $\{\boldsymbol{q}_d, \boldsymbol{\omega}_d, \dot{\boldsymbol{\omega}}_d\}$ denote the desired orientation. The control input of the position tracking can be expressed as:

$$\boldsymbol{y}_p = \ddot{\boldsymbol{p}}_d - \mathbf{K_d}(\dot{\boldsymbol{p}} - \dot{\boldsymbol{p}}_{\mathbf{d}}) - \mathbf{K_p}(\boldsymbol{p} - \boldsymbol{p}_{\mathbf{d}}) \tag{26}$$

where $\mathbf{K}_p, \mathbf{K}_d$ are diagonal positive definite matrices.

The tracking error between the real attitude $\boldsymbol{q} = (a_0, \boldsymbol{\eta}_a)$ and the target attitude $\boldsymbol{q}_d = (b_0, \boldsymbol{\eta}_b)$ can be written as

$$\delta \boldsymbol{q} = \begin{bmatrix} \delta q_0 \\ \delta \boldsymbol{\eta} \end{bmatrix} = \begin{bmatrix} a_0 & -\boldsymbol{\eta}_a{}^T \\ \boldsymbol{\eta}_a & a_0 \mathbf{I}_3 + \boldsymbol{\eta}_a{}^\times \end{bmatrix} \begin{bmatrix} b_0 \\ -\boldsymbol{\eta}_b \end{bmatrix} \tag{27}$$

Then, the control input of the attitude tracking can be expressed as:

$$\boldsymbol{y}_\omega = \dot{\boldsymbol{\omega}}_d - \mathbf{K_2}(\boldsymbol{\omega} - \boldsymbol{\omega_d}) - \mathbf{K_1}\delta\boldsymbol{\eta} \tag{28}$$

where $\mathbf{K}_1, \mathbf{K}_2$ are diagonal positive definite matrices.

V. Simulation Results

In this section, two simulation results are proposed to verify the feasibility of the design concept and the effectiveness of the control algorithm. The simulation model is built by Matlab-Simulink, in which the 3D mechanical systems is constructed using Simscape-Multibody toolbox. We import the complete aerial vehicle CAD assemblies into the model. An automatically generated 3D animation enables visualization of the system dynamics.

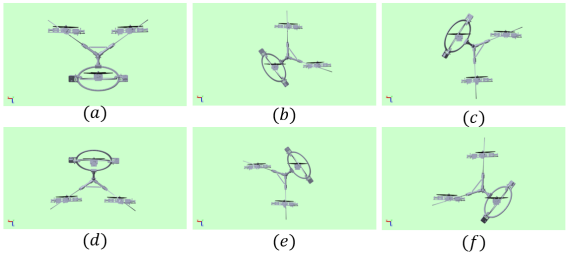

Fig. 5. Simulation diagram for omnidirectional movement.

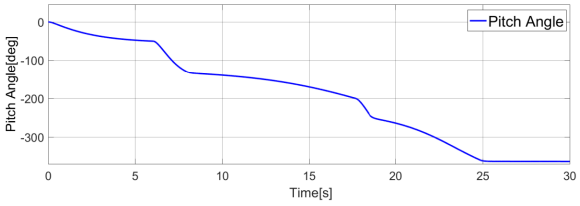

Fig. 6. Real-time angle for omnidirectional movement.

A. Omnidirectional Movement Simulation

The first simulation is an omnidirectional motion test. The robot rotates about Y_B-axis in a horizontal plane. In order to avoid multiple solutions and singularity problems, the control target decomposed into six sub-target values.

In Fig.5, (a)...(f) sequentially represents the 2-DoF tilting modules state of the aerial robot at different positions during the rotation of 360 degrees. Each state of the robot shown in Fig.5. Fig.6 shows the relationship between time and the angle of rotation of the aerial robot. The change in the slope of the curve is due to the position change of the 2-DoF tilting module during the rotation resulting in a change of the control allocation.

B. "8" shaped trajectory tracking

In the second simulation experiment, the mission of the aircraft is to track the plane "8"-shaped trajectory $p_d(t) = \{x_d(t), y_d(t), z_d(t)\}$, and to ensure that the attitude of the body is always in the horizontal state $\omega_d = \begin{bmatrix} 0 & 0 & 0 \end{bmatrix}^{\mathrm{T}}$, and the corresponding expected trajectory is

$$\begin{cases} x_d = 0.5\sin(0.135t) \\ y_d = 0.7\sin(0.27t) \\ z_d = 1 \end{cases} \tag{29}$$

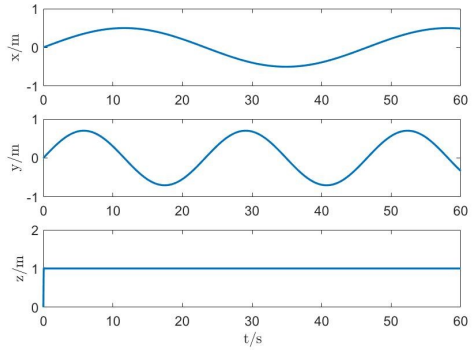

Fig. 7. Real-time location in trajectory tracking.

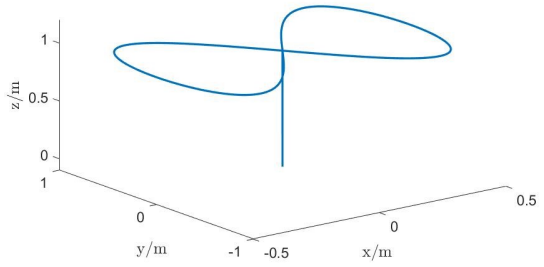

Fig. 8. The Trajectory in 3D space.

The initial position and initial attitude of the aircraft are defined as

$$\begin{cases} [x(0),\ y(0),\ z(0)] = [0\ \ 0\ \ 0] \\ [\phi(0),\ \ \theta(0),\ \ \psi(0)] = [0\ \ 0\ \ 0] \end{cases} \tag{30}$$

Fig.7 shows the real-time position of $x(t), y(t), z(t)$ in the trajectory tracking simulation. It can be seen that the positions

of $x(t)$ and $y(t)$ vary according to a sinusoid, and the position coincides with the desired trajectory. The maximum position tracking error is stable within $0.25mm$. One of the reasons resulting in these errors is that the gyro moment and the rotation of the servo motor are neglected. But the impact of this value is negligible for the actual system, and the control algorithm still applies.

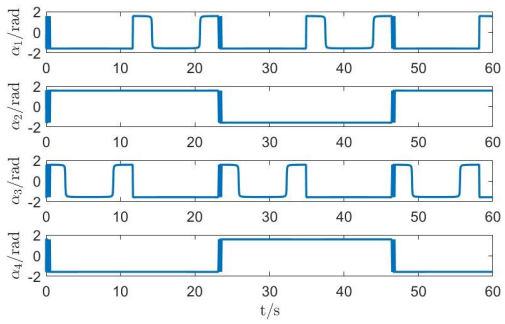

Fig. 9. Tilting angles of 2-DOF tilting modules.

As shown in Fig.8, the real-time trajectory of the aerial vehicle from takeoff to completion of the "8" shaped trajectory tracking task is shown. It can be seen from Fig.9, the change of the tilting angles α_i, and has $\alpha_1 = \beta_3, \alpha_2 = \beta_4, \alpha_3 = \beta_2, \alpha_4 = \beta_2$. The simulation results prove that the designed controller can control the aerial vehicle to complete complex trajectory tracking tasks.

VI. Conclusion

In this manuscripts, a bioinspired novel multi-rotor aerial robot (BioTetra) is presented. Through the analysis of the structure and stability of the molecules CH_4, the design concept of a three-dimensional actuators configuration is proposed. Dynamics modeling, preliminary control design and simulation based on Simscape-Multibody toolbox are also represented. Simulation results verified feasibility of the design approach and the robot's capability to independently control its position and attitude. Future work includes the development of a control allocation capable of adapting the rotor failures.

References

[1] Pratap Tokekar, Joshua Vander Hook, David Mulla, Volkan Isler,"Sensor Planning for a Symbiotic UAV and UGV System for Precision Agriculture", IEEE Transactions on Robotics Volume: 32 , Issue: 6 , Dec. 2016.

[2] Paulo G. de Barros and RobertW. Lindeman, "Multi-sensory urban search-and-rescue robotics: improving the operators omni-directional perception", ROBOTICS AND AI,10.3389/frobt.2014.00014

[3] Hon Ming Yip , Kin Kwan Ho , Man Hin Anson Chu , King W. C. Lai, "Development of an omnidirectional mobile robot using a RGB-D sensor for indoor navigation" The 4th Annual IEEE International Conference on Cyber Technology in Automation, Control and Intelligent,09 October 2014, 10.1109/CYBER.2014.6917454

[4] Prerna Jain1, Pallavi N. Firke2, Kalyanee N. Kapadnis3, Trupti S. Patil4, Sonali S. Rode5,"RF Based Spy Robot "Kalyanee N. Kapadnis et al Int. Journal of Engineering Research and Applications,ISSN : 2248-9622, Vol. 4, Issue 4(Version 2), April 2014, pp.06-09.

[5] D. Brescianini and R. D'Andrea, "Design, modeling and control of an omni-directional aerial vehicle," 2016 IEEE International Conference on Robotics and Automation (ICRA), Stockholm, 2016, pp. 3261-3266.

[6] S. Park, J. Her, J. Kim and D. Lee, "Design, modeling and control of omni-directional aerial robot," 2016 IEEE/RSJ International Conference on Intelligent Robots and Systems (IROS), Daejeon, 2016, pp. 1570-1575.

[7] M. Ryll, G. Muscio, F. Pierri, E. Cataldi, G. Antonelli, F. Caccavale, and A. Franchi, 6d physical interaction with a fully actuated aerial robot, in 2017 IEEE International Conference on Robotics and Automation (ICRA), May 2017, pp. 5190C5195.

[8] Ryll, H. H. Blthoff, and P. R. Giordano, A novel overactuated quadrotor unmanned aerial vehicle: Modeling, control, and experimental validation, IEEE Transactions on Control Systems Technology, vol. 23, no. 2, pp. 540C556, March 2015.

[9] Zhi-Yan Dong, Shun-An Liu, Chao Liu, Jin-Lin Liu, Lei Feng, Modeling and robust control of an unmanned coaxial rotor helicopter with unstructured uncertainties, Advances in Mechanical Engineering, Volume:9 issure:1, Article first published online: January 19, 2017; Issue published: January 1, 2017

[10] Markus Ryll, Heinrich H. Bulthoff, and Paolo Robuffo Giordano, "Modeling and Control of a Quadrotor UAV with Tilting Propellers", IEEE International Conference on Robotics and Automation, 14-18 May 2012, pp.4606-4613.

[11] M. Zhao, T. Anzai, F. Shi, X. Chen, K. Okada and M. Inaba, "Design, Modeling, and Control of an Aerial Robot DRAGON: A Dual-Rotor-Embedded Multilink Robot With the Ability of Multi-Degree-of-Freedom Aerial Transformation," in IEEE Robotics and Automation Letters, vol. 3, no. 2, pp. 1176-1183, April 2018.

[12] Mintchev, Stefano Shintake, Jun Floreano, Dario. (2018). Bioinspired dual-stiffness origami. Science Robotics. 3. eaau0275. 10.1126/scirobotics.aau0275.

[13] Estrada, Matthew Mintchev, Stefano Christensen, David Cutkosky, Mark Floreano, Dario. (2018). Forceful manipulation with micro air vehicles. Science Robotics. 3. eaau6903. 10.1126/scirobotics.aau6903.

[14] Salazar-Cruz S , Kendoul F , Lozano R , et al. Real-time stabilization of a small three-rotor aircraft[J]. IEEE Transactions on Aerospace and Electronic Systems, 2008, 44.

[15] Aravind, P. K . A comment on the moment of inertia of symmetrical solids[J]. American Journal of Physics, 1992, 60(8):754.